ASYMMETRICAL EFFECTS OF BI-ANISOTROPIC SUBSTRATE-SUPERSTRATE SANDWICH STRUCTURE ON PATCH RESONATOR

Chemseddine Zebiri[1, *], Mohamed Lashab[2], and Fatiha Benabdelaziz[3]

[1]Département d'Electronique, Université Ferhat Abbas, Sétif, Route de Béjaia 19000, Algeria

[2]Département de Génie Electrique, Université 20 Août 1955, Skikda 21000, Algeria

[3]Département d'Electronique, Université Mentouri, Constantine 25000, Algeria

Abstract—Few works on symmetric and asymmetric dielectrics have been published, specifically the case of chiral and bi-isotropic media. For this reason and taking into account the complexity of the studied environment, this paper treats the asymmetrical effects on the resonant frequency and the bandwidth of a rectangular microstrip patch antenna in a complex bi-anisotropic substrate-superstrate configuration. This structure is studied theoretically, and the obtained results are discussed and commented. The numerical analysis used in this paper is mainly employed in order to obtain original results. The originality of this work is presented by the bianisotropic chiral asymmetry and the combined effect of the substrate and the superstrate.

1. INTRODUCTION

Earlier publications were focused on understanding how the superstrate affected the resonant frequency and subsequent power matching concerns [1–4]. Other general types of antennas are treated as the multilayered stacked geometry [5], for several patch forms, such as the triangular one [4, 5], rectangular type [5] circular patch [6] and circular annular ring microstrip [7], where the structures with substrate-superstrate are generally employed to improve the characteristics of the resonator, especially those of the antenna [2–4, 6–10].

Several particular cases of such a medium have found practical applications in recent years (chiral materials, biased ferrites, biaxial optical fibers, etc.), and additional applications are likely to occur as a consequence of the introduction of novel synthetic electronic materials [11]. Pozar quoted some disadvantages posed by superstrate, and suggested the most complex mediums, such as biaxial, bi-anisotropic, or the use of an anisotropic superstrate, can have more interesting effects [12]. This suggestion was the subject to use several configurations of the superstrates, and these configurations were used to improve antenna radiation properties, such as dielectric slabs [13, 14], electromagnetic band-gap (EBG) structures [15–20], where Yang et al. [21] were the first who proposed that the antennas with high profit could be obtained by a radiating element printed on EBG, the use of highly-reflective surfaces [10], artificial magnetic [2, 22], effects of self-biased magnetic films on patch antennas with substrate/superstrate sandwich structure [23–28], and bi-anisotropic substrate and superstrates [29, 30].

The improvement brought by anisotropy and thickness of the superstrate is to reduce surface waves resulting in radiation efficiency of more than 90% [1, 24–28, 31], and radar cross section RCS [32–34]. In [35], the authors found the superstrate loaded on the metallic patch can be used for frequency tuning, bandwidth enhancement and RCS reduction.

The idea of using chiral materials as substrates and superstrate in the design of printed antennas was first introduced in 1988 by Engheta [36] and the term 'chirostrip' was then invented, and in 1989, chiroptical guides were invented (and named) by Engheta and Pelet in [37]. These discoveries have opened up a whole new field of theoretical studies on the properties of these guides or resonator-based chiral: new polarizations, crossing patterns, coupling TE/TM wave generation 'slow' resonant frequency, bandwidth and surface wave [38]. It was not until 2001 that the resolution of Maxwell's equations in these structures has been fully completed [39, 40]. And over these years, the interaction of electromagnetic fields with chiral matters has been studied, where the chiral media are used in many applications involving arrays antennas, radomes antenna, microstrip substrates and waveguides [41]. Therefore, it is important to predict the electromagnetic behaviour of a general bi-anisotropic medium. Aside from the fundamental studies contained in [42–44] and related publications, the dispersion relation of such media has been studied in [45], and an application to layered structures has been fully made in [11, 46].

Chiral media are optically active, a behaviour caused by

asymmetrical molecular structure that enables a substance to rotate the plane of incident polarized light, where the amount of rotation in the plane of polarization is proportional to the thickness of the traversed medium as well as to the light wavelength [41, 47–50].

The media can be divided basically into reciprocal [51] and nonreciprocal magneto-electric materials [42, 52, 53]. The most general linear medium is described by bi-anisotropic constitutive relations [42–44]. Note that the constitutive tensors can define whether the medium is reciprocal or not [54], and the effect of this medium in electronic components parameters can be symmetrical or asymmetrical [55, 56].

It should be pointed out that paper [57] is specifically focused on chiral media, i.e., those reciprocal bi-isotropic media whose existence is out of controversy-nonreciprocal bi-isotropic media have neither been found nor manufactured, and the possibility of their existence is currently under discussion in the open literature [58, 59]. The nonreciprocal behaviour of particular classes of such materials has also been studied [11, 60, 61].

In our previous work [29, 30], we studied the effect of chiral substrates and superstrates on the resonant frequencies and bandwidth of microstrip antenna, but in this paper a new effect will be studied, which is the asymmetrical effect of the chirality of the substrates and superstrates on the resonant frequency and bandwidth. Original results are discussed and explained.

2. THEORY

The geometry of superstrate-loaded rectangular microstrip antenna is illustrated in Figure 1. The patch dimensions are $a \times b$ along two axes ox and oy, respectively, which located on a grounded substrate (region 1) of thickness d_1 having the superstrate (region 2) of thickness d_2 on the top. Above the superstrate is a free space (region 3).

The constitutive tensors $\boldsymbol{\varepsilon}$, $\boldsymbol{\mu}$, $\boldsymbol{\xi}$, and $\boldsymbol{\eta}$ of the substrate and superstrate, in this case, are expressed as:

$$\boldsymbol{\varepsilon} = \varepsilon_0 \begin{bmatrix} \varepsilon_t & 0 & 0 \\ 0 & \varepsilon_t & 0 \\ 0 & 0 & \varepsilon_z \end{bmatrix} \tag{1}$$

$$\boldsymbol{\mu} = \mu_0 \begin{bmatrix} \mu_t & 0 & 0 \\ 0 & \mu_t & 0 \\ 0 & 0 & \mu_z \end{bmatrix} \tag{2}$$

$$\boldsymbol{\xi} = \eta = j \begin{bmatrix} 0 & \xi & 0 \\ -\xi & 0 & 0 \\ 0 & 0 & 0 \end{bmatrix} \tag{3}$$
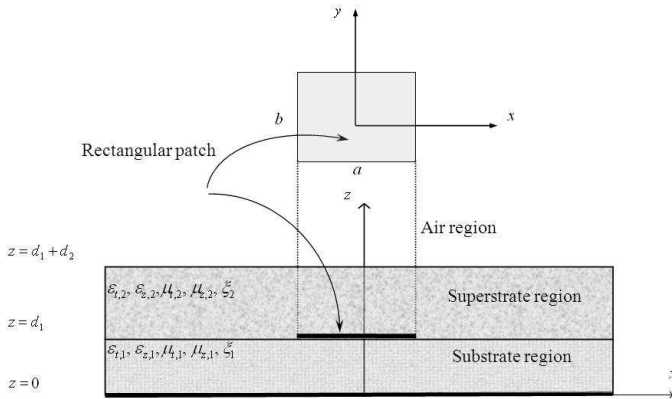
Figure 1. Rectangular microstrip patch antenna in a bi-anisotropic substrate-superstrate configuration.

2.1. Green's Tensor Evaluation

Starting from Maxwell's equations, we can show that the transverse magnetic (e) and transverse electric (h) counterparts of the tangential electric and magnetic fields in the Fourier domain for a bi-anisotropic bounded region having anisotropy tensor of type (3) can be expressed in compact matrix form as follows [29, 30]:

$$\tilde{\mathbf{E}}_s\left(\boldsymbol{\kappa}_s, z\right) = \left[\begin{array}{c} \tilde{E}^e\left(\boldsymbol{\kappa}_s, z\right) \\ \tilde{E}^h\left(\boldsymbol{\kappa}_s, z\right) \end{array}\right] = e^{j\boldsymbol{\kappa}_z z}\mathbf{A}\left(\boldsymbol{\kappa}_s\right) + e^{-j\boldsymbol{\kappa}_z z}\mathbf{B}\left(\boldsymbol{\kappa}_s\right) \tag{4}$$

$$\tilde{\mathbf{H}}_s\left(\boldsymbol{\kappa}_s, z\right) = \left[\begin{array}{c} \tilde{H}^e\left(\boldsymbol{\kappa}_s, z\right) \\ \tilde{H}^h\left(\boldsymbol{\kappa}_s, z\right) \end{array}\right] = e^{j\boldsymbol{\kappa}_z z}\mathbf{g}(\boldsymbol{\kappa}_s)\,\mathbf{A}(\boldsymbol{\kappa}_s) + e^{-j\boldsymbol{\kappa}_z z}\mathbf{h}(\boldsymbol{\kappa}_s)\,\mathbf{B}(\boldsymbol{\kappa}_s) \tag{5}$$

where $\mathbf{A}\left(\boldsymbol{\kappa}_s\right)$ and $\mathbf{B}\left(\boldsymbol{\kappa}_s\right)$ are two-element vectors. Their elements are to be determined by applying the boundary conditions. $\boldsymbol{\kappa}_s = |\boldsymbol{\kappa}_s|$ is the transverse vector wave number and $\boldsymbol{\kappa}_s = \hat{\mathbf{x}}\,\boldsymbol{\kappa}_x + \hat{\mathbf{y}}\boldsymbol{\kappa}_y$.

$$\boldsymbol{\kappa}_z = \sqrt{\boldsymbol{\kappa}_0^2 - \boldsymbol{\kappa}_s^2} \tag{6}$$

$$\boldsymbol{\kappa}_z^e = \sqrt{\boldsymbol{\kappa}_0^2\left(\varepsilon_t\mu_t - \xi^2\right) - \frac{\varepsilon_t}{\varepsilon_z}\boldsymbol{\kappa}_s^2} \tag{7}$$

$$\boldsymbol{\kappa}_z^h = \sqrt{\boldsymbol{\kappa}_0^2\left(\varepsilon_t\mu_t - \xi^2\right) - \frac{\mu_t}{\mu_z}\boldsymbol{\kappa}_s^2} \tag{8}$$

$$\boldsymbol{\kappa}_0 = \sqrt{\omega^2\varepsilon_0\,\mu_0} \tag{9}$$

$$\boldsymbol{\kappa}_s = \sqrt{\boldsymbol{\kappa}_x^2 + \boldsymbol{\kappa}_y^2} \tag{10}$$

$$\mathbf{g}\left(\boldsymbol{\kappa}_s\right) = \mathrm{diag}\left[\begin{array}{cc} \dfrac{\omega\varepsilon_0\varepsilon_t}{j(-\boldsymbol{\kappa}_0\xi+j\boldsymbol{\kappa}_z^e)} & \dfrac{j\left(\boldsymbol{\kappa}_0\xi+j\boldsymbol{\kappa}_z^h\right)}{\omega\mu_0\mu_t} \end{array}\right] \tag{11}$$

$$\mathbf{h}\left(\boldsymbol{\kappa}_s\right) = \mathrm{diag}\left[\begin{array}{cc} \dfrac{\omega\varepsilon_0\varepsilon_t}{j(-\boldsymbol{\kappa}_0\xi-j\boldsymbol{\kappa}_z^e)} & \dfrac{j\left(\boldsymbol{\kappa}_0\xi-j\boldsymbol{\kappa}_z^h\right)}{\omega\mu_0\mu_t} \end{array}\right] \tag{12}$$

$\boldsymbol{\kappa}_z^e$ and $\boldsymbol{\kappa}_z^h$ are respectively the propagation constants for TM and TE waves in the uniaxial dielectric.

Keeping in mind the boundary conditions for the tangential field components in the proximity of the conducting patch, for the structure shown in Figure 1, we are able to derive the relation between the electric source and the electric field in terms of the spectral Green's dyad [30, 62].

$$\mathbf{G}(\boldsymbol{\kappa}_s) = \frac{1}{j\omega\varepsilon}\left[\begin{array}{cc} \dfrac{\left(N_i^e+N_c^e\right)}{\left(D_i^e+D_c^e\right)}N^e\boldsymbol{\kappa}_{z,1}^e & 0 \\ 0 & \dfrac{\left(N_i^h+N_c^h\right)}{\left(D_i^h+D_c^h\right)}\boldsymbol{\kappa}_0^2 \end{array}\right]\sin\left(\boldsymbol{\kappa}_{z,1}d_1\right) \tag{13}$$

$$N^e = \frac{\boldsymbol{\kappa}_0^2\varepsilon_{t,1}\mu_{t,1} - \boldsymbol{\kappa}_s^2\dfrac{\varepsilon_{t,1}}{\varepsilon_{z,1}}}{\boldsymbol{\kappa}_{z,1}^{e2}} \tag{14}$$

$$N_i^e = \boldsymbol{\kappa}_z\cos\left(\boldsymbol{\kappa}_{z,2}^e d_2\right) + j\frac{\boldsymbol{\kappa}_{z,2}^e}{\varepsilon_{t,2}}\sin\left(\boldsymbol{\kappa}_{z,2}^e d_2\right) \tag{15}$$

$$N_c^e = \frac{\boldsymbol{\kappa}_0\xi_2}{\boldsymbol{\kappa}_{z,2}^e}\left(\boldsymbol{\kappa}_z\varepsilon_{t,2} + j\boldsymbol{\kappa}_0\xi_2\right)\sin\left(\boldsymbol{\kappa}_{z,2}^e d_2\right) \tag{16}$$

$$N_i^h = \cos\left(\boldsymbol{\kappa}_{z,2}^h d_2\right) + j\frac{\boldsymbol{\kappa}_z}{\boldsymbol{\kappa}_{z,2}^h}\mu_{t,2}\sin\left(\boldsymbol{\kappa}_{z,2}^h d_2\right) \tag{17}$$

$$N_c^h = -j\frac{\boldsymbol{\kappa}_0\xi_2}{\boldsymbol{\kappa}_{z,2}^h}\sin\left(\boldsymbol{\kappa}_{z,2}^h d_2\right) \tag{18}$$

$$D_i^e = \left(\boldsymbol{\kappa}_z\varepsilon_{t,1}\cos\left(\boldsymbol{\kappa}_{z,1}^e d_1\right) + j\boldsymbol{\kappa}_{z,1}^e\sin\left(\boldsymbol{\kappa}_{z,1}^e d_1\right)\right)\cos\left(\boldsymbol{\kappa}_{z,2}^e d_2\right)$$
$$+j\left(\frac{\varepsilon_{t,1}}{\varepsilon_{t,2}}\boldsymbol{\kappa}_{z,2}^e\cos\left(\boldsymbol{\kappa}_{z,1}^e d_1\right) + j\frac{\boldsymbol{\kappa}_{z,1}^e\boldsymbol{\kappa}_z}{\boldsymbol{\kappa}_{z,2}^e}\varepsilon_{t,2}\sin\left(\boldsymbol{\kappa}_{z,1}^e d_1\right)\right)\sin\left(\boldsymbol{\kappa}_{z,2}^e d_2\right) \tag{19}$$

$$D_c^e = \frac{\boldsymbol{\kappa}_0\xi_1}{\boldsymbol{\kappa}_{z,1}^e}\left(\boldsymbol{\kappa}_z\varepsilon_{t,1} + j\boldsymbol{\kappa}_0\xi_1\right)\sin\left(\boldsymbol{\kappa}_{z,1}^e d_1\right)\cos\left(\boldsymbol{\kappa}_{z,2}^e d_2\right)$$
$$+\frac{\varepsilon_{t,1}}{\varepsilon_{t,2}}\frac{\boldsymbol{\kappa}_0\xi_2}{\boldsymbol{\kappa}_{z,2}^e}\left(\boldsymbol{\kappa}_z\varepsilon_{t,2} + j\boldsymbol{\kappa}_0\xi_2\right)\sin\left(\boldsymbol{\kappa}_{z,2}^e d_2\right)\cos\left(\boldsymbol{\kappa}_{z,1}^e d_1\right)$$
$$+\boldsymbol{\kappa}_0\left(\left(\frac{\varepsilon_{t,1}}{\varepsilon_{t,2}} - \frac{\xi_1}{\xi_2}\right)\frac{\boldsymbol{\kappa}_0\xi_1\xi_2}{\boldsymbol{\kappa}_{z,1}^e\boldsymbol{\kappa}_{z,2}^e}\left(\boldsymbol{\kappa}_z\varepsilon_{t,2}+j\boldsymbol{\kappa}_0\xi_2\right) - j\xi_2\frac{\boldsymbol{\kappa}_{z,1}^e}{\boldsymbol{\kappa}_{z,2}^e} + j\xi_1\frac{\varepsilon_{t,1}}{\varepsilon_{t,2}}\frac{\boldsymbol{\kappa}_{z,2}^e}{\boldsymbol{\kappa}_{z,1}^e}\right)$$
$$\sin\left(\boldsymbol{\kappa}_{z,2}^e d_2\right)\sin\left(\boldsymbol{\kappa}_{z,1}^e d_1\right) \tag{20}$$

$$D_i^h = \frac{1}{\mu_{t,1}} \left[\begin{array}{l} \left(\boldsymbol{\kappa}_{z,1}^h \cos \left(\boldsymbol{\kappa}_{z,1}^h d_1 \right) + j \boldsymbol{\kappa}_z \mu_{t,1} \sin \left(\boldsymbol{\kappa}_{z,1}^h d_1 \right) \right) \cos \left(\boldsymbol{\kappa}_{z,2}^h d_2 \right) \\ + j \left(\mu_{t,2} \frac{\boldsymbol{\kappa}_z \boldsymbol{\kappa}_{z,1}^h}{\boldsymbol{\kappa}_{z,2}^h} \cos \left(\boldsymbol{\kappa}_{z,1}^h d_1 \right) + j \frac{\mu_{t,1}}{\mu_{t,2}} \boldsymbol{\kappa}_{z,2}^h \sin \left(\boldsymbol{\kappa}_{z,1}^h d_1 \right) \right) \sin \left(\boldsymbol{\kappa}_{z,2}^h d_2 \right) \end{array} \right] \quad (21)$$

$$D_c^h = \frac{\boldsymbol{\kappa}_0}{\mu_{t,1}} \left[\begin{array}{l} j \frac{(\xi_2 \mu_{t,1} - \xi_1 \mu_{t,2})(j \boldsymbol{\kappa}_0 \xi_2 - \boldsymbol{\kappa}_z \mu_{t,2})}{\boldsymbol{\kappa}_{z,2}^h \mu_{t,2}} \sin \left(\boldsymbol{\kappa}_{z,1}^h d_1 \right) \sin \left(\boldsymbol{\kappa}_{z,2}^h d_2 \right) \\ + \frac{\boldsymbol{\kappa}_{z,1}^h}{\boldsymbol{\kappa}_{z,2}^h} \xi_2 \sin \left(\boldsymbol{\kappa}_{z,2}^h d_2 \right) \cos \left(\boldsymbol{\kappa}_{z,1}^h d_1 \right) + \xi_1 \cos \left(\boldsymbol{\kappa}_{z,2}^h d_2 \right) \sin \left(\boldsymbol{\kappa}_{z,1}^h d_1 \right) \end{array} \right] \quad (22)$$

$$\boldsymbol{\kappa}_z = \sqrt{\boldsymbol{\kappa}_0^2 - \boldsymbol{\kappa}_s^2} \quad (23)$$

The indices i, c, 1 and 2 respectively represent the uniaxial anisotropic case, chiral case, first layer and second layer.

2.2. Integral Equation Solution

The integral equation describing the electric field on the patch is expressed by application of the boundary condition [63, 64] as:

$$\int\limits_{-\infty}^{\infty} \int d\boldsymbol{\kappa}_s \mathbf{F} \left(\boldsymbol{\kappa}_s, \mathbf{r}_s \right) \cdot \mathbf{G} \left(\boldsymbol{\kappa}_s \right) \cdot \tilde{\mathbf{J}} \left(\boldsymbol{\kappa}_s \right) = 0 \quad (24)$$

The integral equation (24) have to be discritized into matrix equation using the Garlekin procedure of the moment method in Fourier domain, where the surface currents $\mathbf{J}$ on the patch are expanded into a finite series of basis function J_{xn} and J_{ym} according to the following expression:

$$\mathbf{J} \left(\mathbf{r}_s \right) = \sum_{n=1}^{N} a_n \left[\begin{array}{c} J_{xn} \left(\mathbf{r}_s \right) \\ 0 \end{array} \right] + \sum_{m=1}^{M} b_m \left[\begin{array}{c} 0 \\ J_{ym} \left(\mathbf{r}_s \right) \end{array} \right] \quad (25)$$

where, a_n and b_m are the mode expansion coefficients to be sought. We substitute the vector Fourier transform of (25) into (24). Subsequently, the resulting equation is tested by the same set of basis functions used in the expansion of the patch current. Thus, the integral Equation (24) is brought into the following matrix equation:

$$\left[\begin{array}{cc} (\mathbf{B}_1)_{N \times N} & (\mathbf{B}_2)_{N \times M} \\ (\mathbf{B}_3)_{M \times N} & (\mathbf{B}_4)_{M \times M} \end{array} \right] \cdot \left[\begin{array}{c} (\mathbf{a})_{N \times 1} \\ (\mathbf{B})_{M \times 1} \end{array} \right] = \mathbf{0} \quad (26)$$

where, $(\mathbf{B}_1)_{N \times N}$, $(\mathbf{B}_2)_{N \times M}$, $(\mathbf{B}_3)_{M \times N}$ and $(\mathbf{B}_4)_{M \times M}$ are the elements of the digitalized matrix equation.

2.3. Resonant Frequency and Half Power Bandwidth

Equation (26) has a non trivial solution only in the case where the condition below is verified.

$$\det \left(\mathbf{B} \left(\omega \right) \right) = 0 \quad (27)$$

Equation (27) is known as the characteristic equation which has a complex frequency solution such as $f = f_r + if_i$, where f_r is the resonant frequency and f_i the radiation loss in the case of radiating antenna. The quality factor and half power bandwidth are defined in [65, 66] as:

$$Q = \frac{f_r}{2f_i} \tag{28}$$

$$BW = \frac{1}{Q} \tag{29}$$

3. RESULTS

3.1. Combined Effect of the Substrate and Superstrate Chirality (Thin Layer Case)

In the monolayer case [29], the asymmetry effect is more visible when the substrate permittivity $\varepsilon_r = 7$ than in the second case $\varepsilon_r = 2.35$. It is also more apparent on the bandwidth than on the resonant frequency. The increase of layer thickness leads to an increase of the asymmetry effect of the chiral [29].

Figures 2(a)–2(d) and 3(a)–3(d) show the combined effect of the two chiral substrates. Knowing that the substrate thickness $d_1 = 1\,\text{mm}$, in the configuration (substrate/superstrate) case, the asymmetry effect of the substrate is negligible either on the resonant frequency or on the bandwidth, which agrees with the last one [29] and in [30].

Concerning the asymmetry effect, an increase or decrease of the resonant frequency, for a positive magnetoelectric element or negative, is not the same as compared to the isotropic case. The chiral superstrate becomes more important with the increasing of these two factors: the thickness and permittivity (i.e., the asymmetry reaches 1% up to 33% for respectively $\varepsilon_r = 1.5\%$ to $\varepsilon_r = 10$ on the resonant frequency, and on the bandwidth, the asymmetry effect can reach 700% for $\varepsilon_r = 10$).

In the case of the resonant frequency, the asymmetry of the chiral superstrate is important (the effect of the substrate chirality is always negligible due to the weak thickness of this layer), which occurs according to the thickness layers ratio d_2/d_1. For a positive magneto-electric case, there is a monotone increase of the bandwidth. Instead, in the negative magneto-electric case, three zones are observed, the first one located in $0 < d_2/d_1 < 0.5$, where the bandwidth undergoes an increase reaching 100% for all cases. In the second region $0.5 < d_2/d_1 < 1$, the bandwidth undertakes a decrease with the same slope.
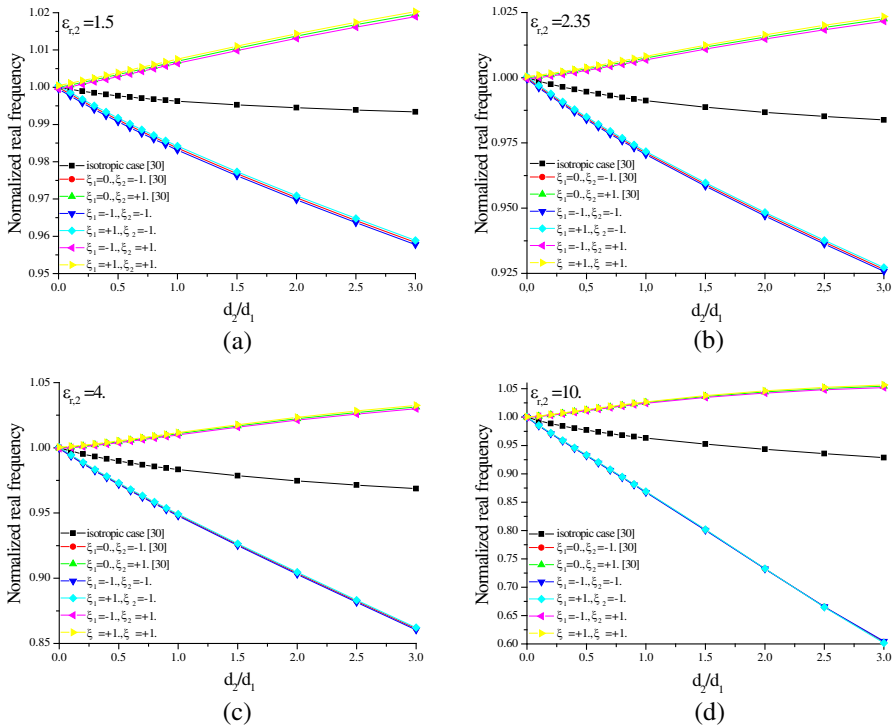
Figure 2. Normalized resonant frequency of a rectangular microstrip patch antenna in a bi-anisotropic substrate-superstrate configuration vs. superstrate thickness; $a = 6\,\text{cm}$, $b = 5\,\text{cm}$, $d_1 = 0.1\,\text{cm}$, $\varepsilon_{t,1} = \varepsilon_{z,1} = 2.35$, $\varepsilon_{z,2} = 1.5, 2.35, 4, 10$.

In the last region $d_2/d_1 > 1$, a monotone increase of the bandwidth is visible.

From the previous section, it is preferable to have the substrate layer thick enough for better observing the combined effect of the both media. Indeed we took $d_1 = 5\,\text{mm}$. The dimensions of the studied structure and ratio d_2/d_1 are preserved such as in the previous cases, and the normalization is compared to the monolayer case ($d_2 = 0$).

3.2. Combined Effect of the Substrate and Superstrate Chirality (Thick Layer Case)

3.2.1. Real Resonant Frequency

Figures 4(a)–4(d) present the associated effect of the two magneto-electric components of the various layers (substrate and superstrate). The behaviour of the real resonant frequency takes the shape studied previously.
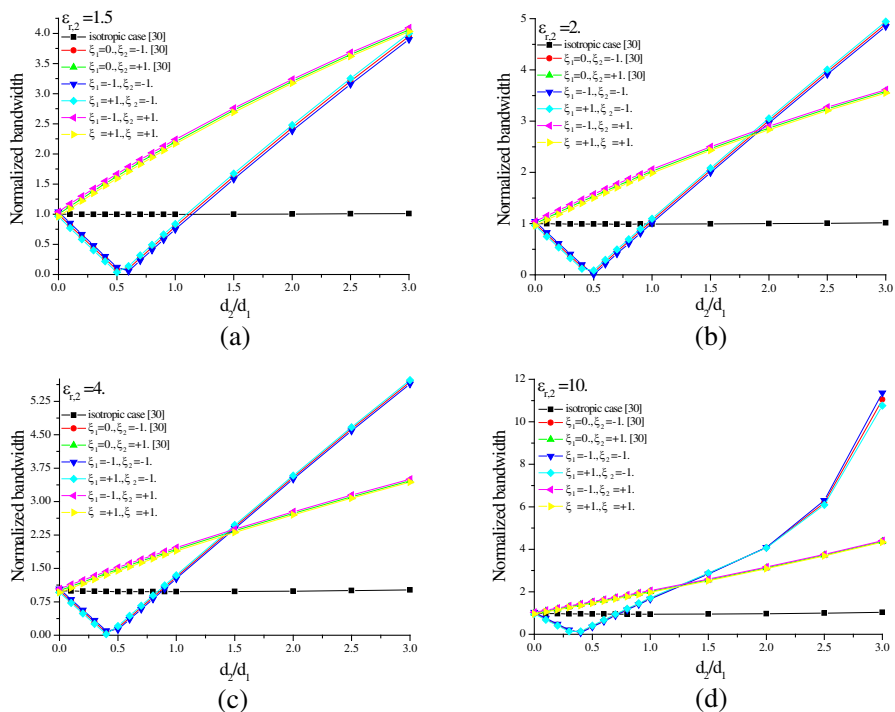
Figure 3. Normalized bandwidth of a rectangular microstrip patch antenna in a bi-anisotropic substrate-superstrate configuration vs. superstrate thickness; $a = 6\,\text{cm}$, $b = 5\,\text{cm}$, $d_1 = 0.1\,\text{cm}$, $\varepsilon_{t,1} = \varepsilon_{z,1} = 2.35$, $\varepsilon_{z,2} = 1.5, 2.35, 4, 10$.

Even with $d_1 = 5\,\text{mm}$, the asymmetry effect of the chiral is not visible, but the combination between the chirality of the substrate and superstrate is asymmetric. By increasing the thickness of the superstrate and its permittivity ε_r, the substrate chirality effect with a negative magnetoelectric element of the superstrate becomes weaker, whereas for a positive chirality of the superstrate, the chirality effect of the substrate is important. The asymmetry effect of the superstrate chirality on the resonant frequency is also remarkable in this case as in the first one.

3.2.2. Bandwidth

Figures 5(a)–5(d) show that the chirality effect of the substrate on the bandwidth is symmetric in this case, but the combined effect (ξ_1
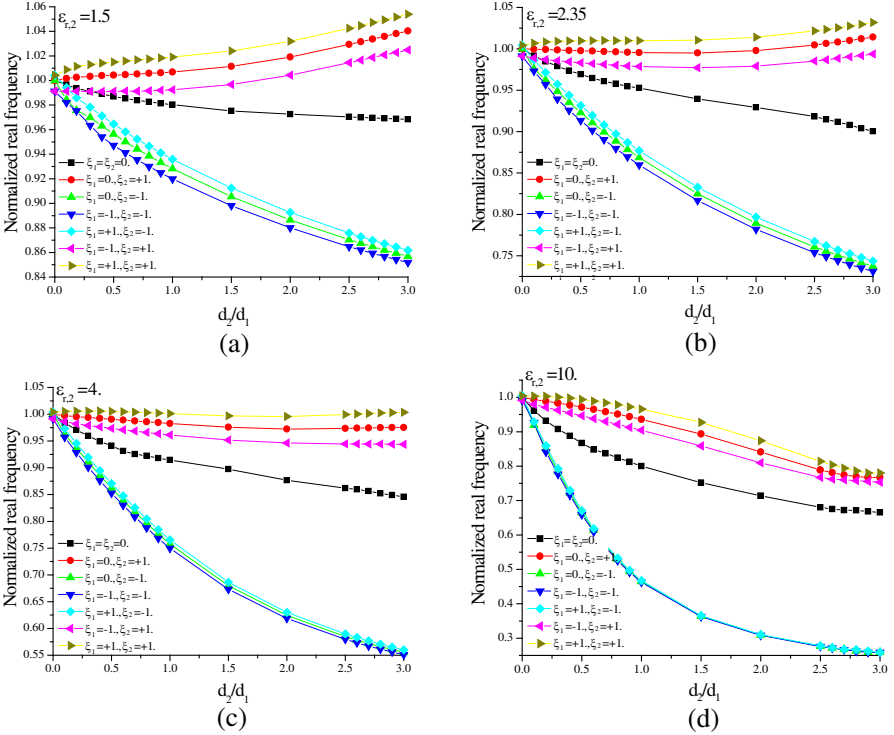
Figure 4. Combined effect of substrate and superstrate on the normalized resonant frequency vs. superstrate thickness; $a = 6\,\text{cm}$, $b = 5\,\text{cm}$, $d_1 = 0.5\,\text{cm}$, $\varepsilon_{t,1} = \varepsilon_{z,1} = 2.35$, $\varepsilon_{z,2} = 1.5, 2.35, 4, 10$.

and ξ_2) is asymmetry on the bandwidth, and it is more apparent for low permittivity ε_r, important ratio d_2/d_1 and for a positive magnetoelectric element of the superstrate ($\xi_2 = +1$, Figures 5(a)–5(b)).

The asymmetry effect of the superstrate chirality on the bandwidth becomes important when increasing both the permittivity ε_r and the thickness of this layer, with a negative magnetoelectric element of the superstrate ($\xi_2 = -1$, Figure 5(d)), whereas in the case of a positive magnetoelectric element of the superstrate, the chirality of the substrate is negligible.

3.3. Interpretation of the asymmetry effect

The symmetry and asymmetry of the bi-isotropic chiral media, having a scalars constitutive parameters, have been reported by some
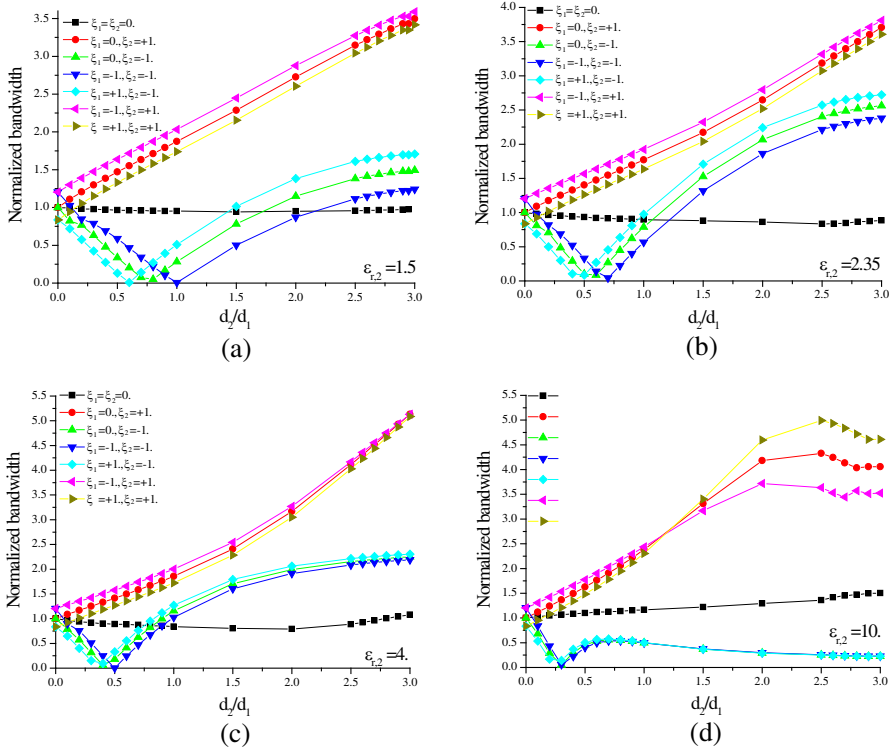
Figure 5. Combined effect of substrate and superstrate on the normalized bandwidth vs. superstrate thickness; $a = 6\,\text{cm}$, $b = 5\,\text{cm}$, $d_1 = 0.5\,\text{cm}$, $\varepsilon_{t,1} = \varepsilon_{z,1} = 2.35$, $\varepsilon_{z,2} = 1.5, 2.35, 4, 10$.

authors [55, 56]. In [55], the authors found that the chiral substrate produces additional longitudinal asymmetric and transverse symmetric field components, only in the case of isotropic study.

This effect could significantly change the properties of microwave devices built on a chiral substrate, and with respect to the asymmetry in this case, it is necessary to evaluate the asymptotic form of the Green tensor. This form is obtained analytically just below, when $d_1 \to 0$, and d_2 maintained constant to show the asymmetry effect of this chiral

layer, according to the Green tensor given in (13) as the following:

$$\mathbf{G}\left(\boldsymbol{\kappa}_s\right) \rightarrow \frac{d_1}{j\omega\varepsilon}$$

$$\begin{bmatrix} \dfrac{\left(\boldsymbol{\kappa}_0^2\varepsilon_{t,1}-\boldsymbol{\kappa}_s^2\right)\left(\boldsymbol{\kappa}_z\cos\left(\boldsymbol{\kappa}_{z,2}^e d_2\right)+\left(j\frac{\boldsymbol{\kappa}_{z,2}^e}{\varepsilon_{t,2}}+\frac{\boldsymbol{\kappa}_0\xi_2}{\boldsymbol{\kappa}_{z,2}^e}\left(\boldsymbol{\kappa}_z\varepsilon_{t,2}+j\boldsymbol{\kappa}_0\xi_2\right)\right)\sin\left(\boldsymbol{\kappa}_{z,2}^e d_2\right)\right)}{\left(\boldsymbol{\kappa}_z\varepsilon_{t,1}\cos\left(\boldsymbol{\kappa}_{z,2}^e d_2\right)+j\left(\boldsymbol{\kappa}_{z,2}^e\sin\left(\boldsymbol{\kappa}_{z,2}^e d_2\right)-j\frac{\varepsilon_{t,1}}{\varepsilon_{t,2}}\frac{\boldsymbol{\kappa}_0\xi_2}{\boldsymbol{\kappa}_{z,2}^e}\left(\boldsymbol{\kappa}_z\varepsilon_{t,2}+j\boldsymbol{\kappa}_0\xi_2\right)\right)\sin\left(\boldsymbol{\kappa}_{z,2}^e d_2\right)\right)} & 0 \\ 0 & \boldsymbol{\kappa}_0^2 \end{bmatrix}$$

$$\tag{30}$$

It can be noticed form the previous expression that the chirality anomaly is observed as:

$$\mathbf{G}^e\left(\boldsymbol{\kappa}_s\right) \rightarrow f\left(\frac{\boldsymbol{\kappa}_0}{\boldsymbol{\kappa}_{z,2}^e}\left(\boldsymbol{\kappa}_z\varepsilon_{t,2}\xi_2+j\boldsymbol{\kappa}_0\xi_2^2\right)\sin\left(\boldsymbol{\kappa}_{z,2}^e d_2\right)\right) \tag{31}$$

The term $\left(\varepsilon_{t,2}\xi_2\sin\left(\boldsymbol{\kappa}_{z,2}^e d_2\right)\right)$ is significant for important value of $\varepsilon_{t,2}$. This last result can explain some previous results in this paper.

This anomaly can be explained also by the fact that the fields are divided into the symmetric and asymmetric field components. The symmetric field components were only slightly affected by the chirality of the media, but the asymmetric field components were affected entirely due to the chirality of the media.

This can be clearly noticed by rewriting the equations, TE and TM immitance in symmetric and asymmetric forms:

$$\mathbf{g}\left(\boldsymbol{\kappa}_s\right) = \mathrm{diag}\left[\underbrace{j\frac{\omega\varepsilon_0\varepsilon_t\boldsymbol{\kappa}_0\xi}{\left(\boldsymbol{\kappa}_0^2\xi^2+\boldsymbol{\kappa}_z^{e2}\right)}}_{\text{asymmetric part}}+\underbrace{j\boldsymbol{\kappa}_z^e\frac{\omega\varepsilon_0\varepsilon_t}{\left(\boldsymbol{\kappa}_0^2\xi^2+\boldsymbol{\kappa}_z^{e2}\right)}}_{\text{symmetric part}} \quad \underbrace{\frac{j\left(\boldsymbol{\kappa}_0\xi+j\boldsymbol{\kappa}_z^h\right)}{\omega\mu_0\mu_t}}_{\text{asymmetric part}}\right] \tag{32}$$

$$\mathbf{h}\left(\boldsymbol{\kappa}_s\right) = \mathrm{diag}\left[\underbrace{j\frac{\omega\varepsilon_0\varepsilon_t\boldsymbol{\kappa}_0\xi}{\left(\boldsymbol{\kappa}_0^2\xi^2+\boldsymbol{\kappa}_z^{e2}\right)}}_{\text{asymmetric part}}-\underbrace{j\boldsymbol{\kappa}_z^e\frac{\omega\varepsilon_0\varepsilon_t}{\left(\boldsymbol{\kappa}_0^2\xi^2+\boldsymbol{\kappa}_z^{e2}\right)}}_{\text{symmetric part}} \quad \underbrace{\frac{j\left(\boldsymbol{\kappa}_0\xi-j\boldsymbol{\kappa}_z^h\right)}{\omega\mu_0\mu_t}}_{\text{asymmetric part}}\right] \tag{33}$$

The asymmetric part occurs in the TE and TM immitance Equations (32) and (33) according to the sign of the magnetoelectric element ξ. And contrary to the case studied in [55], according to the noted preceding remarks, and taking account the Equation (3), which shows a gyrotropic form of the bi-anisotropic media, this non-diagonal shape of the magnetoelectric element produces an asymmetry in the longitudinal component and the component transverses.

In addition, according to our observations, it was found that the layer thickness has an effect on the Chiral asymmetry, where the variation of the layer leads to a variation of the transverses components.

4. CONCLUSION

The numerical results for resonant frequency and bandwidth were presented for different values of constitutive parameters. The asymmetric effect of thin chiral substrate is negligible in the first case (monolayer microstrip antenna), but the effect of the superstrate is always important.

Also another interesting and original result was obtained, which is not discussed in the literature, and it is the relationship between the permittivity (exactly $\varepsilon_{t,2}$) and the chiral constitutive parameter, as given previously. It has been noticed that by increasing the permittivity, the asymmetrical effect of the chiral becomes high, and for complex values of the magneto-electric parameters $\boldsymbol{\xi}$, $\boldsymbol{\eta}$ (in this case a non-diagonal matrix) has shown that the transverse component occurs in the chiral asymmetry, which is not the case for bi-isotropic case study where $\boldsymbol{\xi}$, $\boldsymbol{\eta}$ have a scalar form. In addition to what is given in the literature, it was found that the layer plays an important role in the chiral asymmetry.

In conclusion, we must bear in mind that the bi-anisotropy and specially the asymmetry of the substrates should always be kept into account in the design of the microstrip resonators. Furthermore, to improve the resonator parameters, the chiral is probably the most convenient for this task, since this artificial medium can be modelled as requested.

REFERENCES

1. Ramahi, O. M. and Y. T. Lo, "Superstrate effect on the resonant frequency of microstrip antennas," *Microwave and Optic. Tech. Letts.*, Vol. 5, No. 6, 2540–257, 1992.

2. Attia, H., L. Yousefi, and O. M. Ramahi, "Analytical model for calculating the radiation field of microstrip antennas with artificial magnetic superstrates: Theory and experiment," *IEEE Trans. Antennas Propagat.*, Vol. 59, No. 5, 1438–1445, 2011.

3. Alexopoulos, N. G. and D. R. Jackson, "Fundamental superstrate (cover) effects on printed circuit antennas," *IEEE Trans. Antennas Propagat.*, Vol. 32, No. 8, 807–816, 1984.

4. Biswas, M. and D. Guha, "Input impedance and resonance characteristic of superstrate loaded triangular microstrip patch," *IET Microwaves, Antennas Propagat.*, Vol. 3, No. 1, 92–98, 2009.

5. Mirshekar-Syankal, D. and H. R. Hassani, "Characteristics of stacked rectangular and triangular patch antennas for dual band

application," *8th IEE Int. Conf. Antennas and Propagat.*, Vol. 2, 728–731, 1993.

6. Guha, D. and J. Y. Siddiqui, "Resonant frequency of circular microstrip antenna covered with dielectric superstrate," *IEEE Trans. Antennas Propagat.*, Vol. 51, No. 7, 1649–1652, 2003.

7. Shinde, J., P. Shinde, R. Kumar, M. D. Uplane, and B. K. Mishra, "Resonant frequencies of a circularly polarized nearly circular annular ring microstrip antenna with superstrate loading and airgaps," *Kaleidoscope: Beyond the Internet? — Innovations for Future Networks and Services, 2010 ITU–T*, 1–7, Dec. 13–15, 2010.

8. Foroozesh, A. and L. Shafai, "Effects of artificial magnetic conductors in the design of low-profile high-gain planar antennas with high permittivity dielectric superstrate," *IEEE Antenna Wireless Propagat. Lett.*, Vol. 8, 10–13, 2009.

9. Valagiannopoulos, C. A. and N. L. Tsitsas, "On the resonance and radiation characteristics of multi-layered spherical microstrip antennas," *Electromagnetics*, Vol. 28, No. 4, 243–264, 2008.

10. Foroozesh, A. and L. Shafai, "Investigation into the effects of the patch type FSS superstrate on the high-gain cavity resonance antenna design," *IEEE Trans. Antennas Propagat.*, Vol. 58, No. 2, 258–270, 2010.

11. Uslenghi, P. L. E., "TE-TM decoupling for guided propagation in bianisotropic media," *IEEE Trans. Antennas Propagat.*, Vol. 45, No. 2, 284–286, 1997.

12. Pozar, D. M., "Radiation and scattering from a microstrip patch on a uniaxial substrate," *IEEE Trans. Antennas Propagat.*, Vol. 35, No. 6, 613–621, 1987.

13. Vettikalladi, H., O. Lafond, and M. Himdi, "High-efficient and high-gain superstrate antenna for 60-GHz indoor communication," *IEEE Antenna Wireless Propagat. Lett.*, Vol. 8, 1422–1425, 2009.

14. Mittra, R., Y. Li, and K. Yoo, "A comparative study of directivity enhancement of microstrip patch antennas with using three different superstrates," *Microwave and Optic. Tech. Letts.*, Vol. 52, No. 2, 327–331, 2010.

15. Lee, Y. J., J. Yeo, R. Mittra, and W. S. Park, "Application of electromagnetic bandgap (EBG) superstrates with controllable defects for a class of patch antennas as spatial angular filters," *IEEE Trans. Antennas Propagat.*, Vol. 53, No. 1, 224–235, 2005.

16. Attia, H. and O. M. Ramahi, "EBG superstrate for gain and bandwidth enhancement of microstrip array antennas," *Proceeding*

of IEEE AP-S Int. Symp. Antennas Propagat., 1–4, San Diego, CA, 2008.

17. Korkontzila, E. G., D. B. Papafilippou, and D. P. Chrissoulidis, "Miniaturization of microstrip patch antenna for wireless applications by use of multilayered electromagnetic band gap substrate," *1st European Conference on Antennas and Propagat., EuCAP*, 1–6, 2006.

18. Jha, K. R. and G. Singh, "Microstrip patch antenna on photonic crystal substrate at terahertz frequency," *Applied Electromagnetics Conference (AEMC)*, 1–4, 2009.

19. De, A., N. S. Raghava, S. Malhotra, P. Arora, and R. Bazaz, "Effect of different substrates on compact stacked square microstrip antenna," *Journal of Telecommunications*, Vol. 1, No. 1, 63–65, Feb. 2010.

20. Boutayeb, H. and T. A. Denidni, "Gain enhancement of a microstrip patch antenna using a cylindrical electromagnetic crystal substrate," *IEEE Trans. Antennas Propagat.*, Vol. 55, No. 11, 3140–3145, 2007.

21. Yang, H. Y. D., N. G. Alexopoulos, and E. Yablonovitch, "Photonic band gap materials for high gain printed circuit antennas," *IEEE Trans. Antennas Propagat.*, Vol. 45, No. 1, 185–187, 1997.

22. Attia, H., L. Yousefi, O. Siddiqui, and O. M. Ramahi, "Analytical formulation of the radiation field of printed antennas in the presence of artificial magnetic superstrates," *Applied Physics A*, Vol. 103, No. 3, 877–880, 2011.

23. Yang, G. M., X. Xing, O. Obi, A. Daigle, M. Liu, S. Stoute, K. Naishadham, and N. X. Sun, "Loading effects of self–biased magnetic films on patch antennas with substrate/superstrate sandwich structure," *IET Microwaves, Antennas Propagat.*, Vol. 4, No. 9, 1172–1181, 2010.

24. Dixit, L. and P. K. S. Pourush, "Radiation characteristics of switchable ferrite microstrip array antenna," *IEE Proc. Microwave and Antennas Propagat.*, Vol. 147, No. 2, 151–155, 2000.

25. Batchelor, J. C. and R. J. Langley, "Beam scanning using microstrip line on biased ferrite," *Electronic Lett.*, Vol. 33, No. 8, 645–646, 1997.

26. Ufimtsev, P. Y., R. T. Ling, and J. D. Scholler, "Transformation of surface waves in homogenous absorbing layers," *IEEE Trans. Antennas Propagat.*, Vol. 48, No. 2, 214–222, 2000.

27. Horsfield, B. and J. A. R. Ball, "Surface wave propagation on a

grounded dielectric slab covered by a high–permittivity material,"
IEEE Microwave and Guided Wave Letters, Vol. 10, No. 5, 171–
173, 2000.

28. Saxena, N. K., N. Kumar, and P. K. S. Pourush, "Microstrip rect-
angular patch antenna printed on liti ferrite with perpendicular
DC magnetic biasing," *The Journal of American Science*, Vol. 6,
No. 3, 46–52, 2010.

29. Zebiri, C., M. Lashab, and F. Benabdelaziz, "Effect of anisotropic
magneto-chirality on the characteristics of a microstrip resonator,"
IET Microwaves, Antennas Propagat., Vol. 4, No. 4, 446–452,
2010.

30. Zebiri, C., M. Lashab, and F. Benabdelaziz, "Rectangular
microstrip antenna with uniaxial bi-anisotropic chiral substrate-
superstrate," *IET Microwaves, Antennas Propagat.*, Vol. 5, No. 1,
17–29, 2011.

31. Liu, D., H. C. Chen, and B. Floyd, "An LTCC superstrate
patch antenna for 60-GHz package applications," *IEEE Antennas
and Propagat. Society International Symposium (APSURSI)*, 1–4,
2010.

32. Wu, B.-I., W. Wang, J. Pacheco, X. Chen, T. M. Grzegorczyk, and
J. A. Kong, "A study of using metamaterial as antenna substrate
to enhance gain," *Progress In Electromagnetics Research*, Vol. 51,
295–328, 2005.

33. Jackson, D. R., "The RCS of a rectangular microstrip patch
in a substrate-superstrate geometry," *IEEE Trans. Antennas
Propagat.*, Vol. 38, No. 1, 2–8, 1990.

34. Wang, S., X. Guan, D. Wang, X. Ma, and Y. Su, "Electromagnetic
scattering by mixed conducting/dielectric objects using higher
order MOM," *Progress In Electromagnetics Research*, Vol. 66, 51–
63, 2006.

35. Thakare, Y. B. and Rajkumar, "Design of fractal patch antenna
for size and radar cross-section reduction," *IET Microwaves,
Antennas Propagat.*, Vol. 4, No. 2, 175–181, 2010.

36. Engheta, N., "The theory of chirostrip antennas," *Proceedings
of the 1988 URSI International Radio Science Symposium*, 213,
Syracuse, New York, 1988.

37. Engheta, N. and P. Pelet, "Modes in chirowaveguides," *Optics
Letters*, Vol. 14, No. 11, 593–595, 1989.

38. Engheta, N. and P. Pelet, "Reduction of surface waves in
chirostrip antennas," *Electronics Letters*, Vol. 27, No. 1, 5–7, 1991.

39. Herman, W.-N., "Polarization eccentricity of the transverse field

for modes in chiral core planar waveguides," *Journal of the Optical Society of America A: Optics, Image Science and Vision*, Vol. 18, No. 11, 2806–2818, 2001.

40. Bahar, E., "Mueller matrices for waves reflected and transmitted through chiral materials: Waveguide modal solutions and applications," *Journal of the Optical Society of America B*, Vol. 24, No. 7, 1610–1619, 2007.

41. Al Sharkawy, M., A. Z. Elsherbeni, and S. F. Mahmoud, "Electromagnetic scattering from parallel chiral cylinders of circular cross sections using an iterative procedure," *Progress In Electromagnetics Research*, Vol. 47, 87–110, 2004.

42. Kong, J. A., *Electromagnetic Waves Theory*, EMW Publishing, Cambridge, MA, USA, 2005.

43. Yang, H.-Y. and P. L. E. Uslenghi, "Planar bianisotropic waveguides," *Radio Science*, Vol. 28, No. 5, 919–927, 1993.

44. O'Dell, T. H., *The Electrodynamics of Magnetoelectric Media*, Amsterdam, North-Holland, 1970.

45. Graglia, R. D., P. L. E. Uslenghi, and R. E. Zich, "Dispersion relation for bianisotropic materials and its symmetry properties," *IEEE Trans. Antennas Propagat.*, Vol. 39, No. 1, 83–90, 1991.

46. Graglia, R. D., P. L. E. Uslenghi, and R. E. Zich, "Reflection and transmission for planar structures of bianisotropic media," *Electromagnetics*, Vol. 11, 193–208, 1991.

47. Al-Kanhal, M. A. and E. Arvas, "Electromagnetic scattering from a chiral cylinder of arbitrary cross section," *IEEE Trans. Antennas Propagat.*, Vol. 44, No. 7, 1041–1048, 1996.

48. Engheta, N. and D. L. Jaggard, "Electromagnetic chirality and its applications," *IEEE Antennas Propagat. Soc. Newsletter*, Vol. 30, No. 5, 6–12, 1988.

49. Mahmoud, S. F., "Mode characteristics in chirowaveguides with constant impedance walls," *Journal of Electromagnetic Waves and Applications*, Vol. 6, Nos. 5–6, 625–640, 1992.

50. Graglia, R. D., P. L. E. Uslenghi, and C. L. Yu, "Electromagnetic oblique scattering by a cylinder coated with chiral layers and anisotropic jump-admittance sheets," *Journal of Electromagnetic Waves and Applications*, Vol. 6, No. 1, 695–719, 1992.

51. Sheng, X. Q. and Y. Ekn, "Analysis of microstrip antennas on finite chiral substrates," *International Journal of RF and Microwave Computer-aided Engineering*, Vol. 14, No. 1, 49–56, 2004.

52. Kamenetskii, E. O., "Nonreciprocal microwave bianisotropic

materials: Reciprocity theorem and network reciprocity," *IEEE Trans. Antennas Propagat.*, Vol. 49, No. 3, 361–366, 2001.

53. Serdyukov, A., I. Semchenko, S. Tretyakov, and A. Sihvola, *Electromagnetics of Bi-anisotropic Materials: Theory and Applications*, Taylor & Francis, 2001.

54. Cheng, X., J. A. Kong, and L. Ran, "Polarization of waves in reciprocal and nonreciprocal uniaxially bianisotropic media," *PIERS Online*, Vol. 4, No. 3, 331–335, 2008.

55. Kluskens, M. S. and E. H. Newman, "A microstrip line on a chiral substrate," *IEEE Transactions on Microwave Theory and Techniques*, Vol. 39, No. 11, 1889–1891, 1991.

56. Kluskens, M. S. and E. H. Newman, "Method of moments analysis of scattering by chiral media," Defense Technical Information Center, Ft. Belvoir, 1991.

57. Plaza, G., F. Mesa, and M. Horno, "Study of the dispersion characteristics of planar chiral lines," *IEEE Transactions on Microwave Theory and Techniques*, Vol. 46, No. 8, 1150–1157, 1998.

58. Lakhtakia, A. and W. Weiglhofer, "Constraint on linear, spatiotemporally nonlocal, spatiotemporally nonhomogenous constitutive relations," *International Journal of Infrared and Millimeter Waves*, Vol. 17, No. 11, 1867–1878, 1996.

59. Krowne, C. M., "Demonstration of marginal nonreciprocity in linear bi-isotropic material and comparison to ferrite material," *Proc. Bianisotropics'97, Int. Conf. and Workshop Electromagnetics Complex Media*, 261–264, Glasgow, Scotland, 1997.

60. Uslenghi, P. L. E., "Theory of certain bianisotropic waveguides," *Proc. URSI Int. Symp. Electromagnetic Th. Proc.*, 293–295, Sydney, Australia, 1992.

61. Yang, H.-Y. and P. L. E. Uslenghi, "Planar bianisotropic waveguides," *Radio Science*, Vol. 28, No. 5, 919–927, 1993.

62. Toscano, A. and L. Vegni, "Analysis of printed-circuit antennas with chiral substrates with the method of lines," *IEEE Trans. Antennas Propagat.*, Vol. 49, No. 1, 48–54, 2001.

63. Wong, K.-L., J.-S. Row, C.-W. Kuo, and K.-C. Huang, "Resonance of a rectangular microstrip patch on a uniaxial substrate," *IEEE Transactions on Microwave Theory and Techniques*, Vol. 41, 698–701, Apr. 1993.

64. Bouttout, F., F. Benabdelaziz, T. Fortaki, and D. Khedrouche, "Resonant frequency and bandwidth of a superstrate-loaded rect-

angular patch on a uniaxial anisotropic substrate," *Communications in Numerical Methods in Engineering*, Vol. 16, No. 7, 459–473, John Wiley & Sons, Jul. 2000.

65. Pozar, D. M., "General relations for a phased array of printed antennas derived from infinite current sheets," *IEEE Trans. Antennas Propagat.*, Vol. 33, 498–504, May 1985.

66. Harokopus, W. P., L. P. B. Katehi, W. Y. Ali-Ahmed, and G. M. Rebiez, "Surface wave excitation from open microstrip discontinuities," *IEEE Transactions on Microwave Theory and Techniques*, Vol. 39, 1098–1107, Jul. 1991.